

# Efficient embedding with different time delays

Sara P. Garcia\*

*Instituto de Tecnologia Química e Biológica, Universidade Nova de Lisboa,  
Rua da Quinta Grande 6, 2780-156 Oeiras, Portugal*

Jonas S. Almeida

*Department of Biostatistics, Bioinformatics and Epidemiology,  
Medical University of South Carolina,  
135 Cannon Street, Charleston, SC 29425, USA*

(Dated: December 2, 2024)

## Abstract

An efficient selection of time delays for phase space reconstruction is proposed and compared to the standard use of time delayed mutual information. This novel procedure is based on nearest neighbor estimations and on allowing different time delays for consecutive embedding dimensions. A case study of numerically generated solutions of the Lorenz system contaminated with various levels of Gaussian white noise is used for illustration. A heuristic is suggested to cope with the effect of noise.

PACS numbers: 05.45.Tp, 05.40.Ca

Reconstructing the phase space of a dynamical system from a time series is a well-known mathematical result, central to almost all nonlinear time series analysis methods (see [1, 2] for a general introduction). It is of paramount importance as it ensures that, under certain generic conditions, such a reconstruction is equivalent to the original phase space. This equivalence ensures that differential information is preserved, and allows for both qualitative and quantitative analysis of the dynamical system. Phase space reconstruction by time delay embedding implies estimating a matrix of delay-coordinate vectors, from either scalar or multivariate measurements. To optimize such a matrix, two parameters need to be estimated. The first is the time delay  $\tau$ , which quantifies the time displacement between successive delay-coordinate vectors. The second is the embedding dimension  $m$ , which quantifies the number of such delay-coordinate vectors. We address the problem of estimating the first parameter, the time delay, by suggesting a novel procedure and comparing it to the standard use of time delayed mutual information. The motivation for this study is the increasing interest in characterizing dynamic invariance in biological systems (examples can be found in [3, 4, 5]). Such a goal requires special focus on efficient phase space reconstruction, due to the typically shorter and noisier nature of the data.

Consider a smooth deterministic dynamical system  $s(t) = f(s_{(0)})$ , either in continuous or discrete time, whose trajectories are asymptotic to a compact  $d$ -dimensional manifold  $\mathcal{A}$ . When performing  $k$ -dimensional measurements, a function  $x_{(i)} = h[s(t = i \times \delta)]$ ,  $x \in \mathbb{R}^k$ , where  $\delta$  is the sampling time, relates the states of the dynamical system throughout time  $s(t)$  with a time series of collected points  $x_{(i)}$ . As a consequence of our ignorance on the system, or of limitations of the measurement apparatus, or simply because it is too costly,  $d$ -dimensional measurements are typically not made and therefore  $k \leq d$  [6, 7]. Phase space reconstruction by time delay embedding is a method of generating an  $m$ -dimensional manifold that is equivalent to the original  $d$ -dimensional manifold. In order to do so, an  $m$ -dimensional matrix of delay-coordinate vectors, named embedding matrix, must be built from a vector or a matrix of measurements. The simplest case is when  $k = 1$  and a measurements vector  $\mathbf{x}_{(i)}$  is repeated with displacement to build the embedding matrix  $\mathbf{X} = [\mathbf{x}_{(i)}, \mathbf{x}_{(i+\tau)}, \dots, \mathbf{x}_{(i+(m-1)\tau)}]$ .

In this report, we only address the first part of the phase space reconstruction problem, which considers the estimation of  $\tau$ . Though in the limit of infinite data and infinite precision  $\tau$  may be set to any arbitrary value, a balance between relevance and redundancy [7] must be accomplished for real data. When  $\tau$  is too small, the elements of the delay-coordinate vectors

will mostly be around the bisectrix of the phase space and, consequently, the reconstruction will not be satisfactory. On the contrary, if  $\tau$  is too large the delay-coordinate vectors will become increasingly uncorrelated, with the consequent loss of ability to recover the underlying attractor. In addition, using a time delay larger than necessary will render fewer data points for the reconstruction. This may be particularly limiting for the study of biological systems, where data sets are often not too long. The most common procedure for selecting  $\tau$  is using the first minimum of time delayed mutual information, as proposed by Fraser and Swinney [8]:  $I(x_{(i)}, x_{(i+\tau)}, \tau) = H(x_{(i)}) + H(x_{(i+\tau)}) - H(x_{(i)}, x_{(i+\tau)}) = \sum p(x_{(i)}, x_{(i+\tau)}) \log_2 \frac{p(x_{(i)}, x_{(i+\tau)})}{p(x_{(i)})p(x_{(i+\tau)})}$ , where  $H(x)$  is the Shannon entropy [9]. Nonetheless its widespread use, some drawbacks can be pointed out to this selection criterion. The first is that probabilities are estimated by creating a histogram for the probability distribution of the data, which depends on a heuristic choice of number of bins, for example,  $\log_2$  of the total number of points [10]. Therefore,  $I$  depends on the partitioning. The second drawback is that it contains no dynamical information, which might be incorporated by considering transition rather than static probabilities, but such correction is usually not made [11]. The third is that the selection criterion presented by Fraser and Swinney [8], though generalized to higher dimensions, was established for two-dimensional embeddings [7], and does not necessarily hold for higher dimensional embeddings, as shown below. Finally, a fourth drawback [7] is associated with the fact that, when the purpose is solely to maximize statistical independence [8], there is no obvious reason to choose the first minimum over others.

We propose an alternative measure for selecting time delays, based on nearest neighbor estimations. This nearest neighbor measure  $N$ , is inspired by the false nearest neighbors algorithm  $FNN$  proposed by Kennel *et al.* [12]. With minimal assumptions, this measure is based solely on topological and dynamical arguments documented by the data.

We do not address the second part of the phase space reconstruction problem, which considers the estimation of  $m$ . The embedding theorem proposed by Takens [13] guarantees a solution. It states that if a map from the original  $d$ -dimensional phase space  $\mathcal{A}$ , to the reconstructed  $m$ -dimensional phase space is generic, when  $m \geq (2d + 1)$  that map is a diffeomorphism on  $\mathcal{A}$ , that is, an embedding, or a smooth one-to-one map with a smooth inverse. This one-to-one property implies that if the system is deterministic, distinct points on the attractor  $\mathcal{A}$  are mapped to distinct points under the embedding map [6]. Nevertheless, using the  $FNN$  algorithm (see [12] for an explanation) is common procedure.

The method we propose, based on the nearest neighbor measure  $N$ , introduces three differences to the previously mentioned  $\tau$  selecting procedure  $I$ . The first, is the  $N$  measure *per se*. The second, is being designed to accommodate scalar as well as multivariate measurements, that is, for all  $1 \leq k \leq d$ . And the third difference is using a vector of time delays  $[\tau_1, \tau_2, \dots, \tau_{(m-1)}]$ , for building the embedding matrix  $\mathbf{X} = [\mathbf{x}_{(i)}, \mathbf{x}_{(i+\tau_1)}, \mathbf{x}_{(i+\tau_2)}, \dots, \mathbf{x}_{(i+\tau_{(m-1)})}]$ , here exemplified for the simplest case, when  $k = 1$ . This is justified as using the same  $\tau$  is an assumption out of convenience and not imposed by any theoretical argument [7]. As a consequence, phase space reconstruction will make use of a recursive structure:

for each  $m$

{ for each  $\tau$   
{ estimate  $N$  through steps 1 to 6 (see below) }  
estimate  $FNN$  (algorithm in [12]) }

which will output, for each  $m$ , a vector of the fraction of points that meet our criteria  $N$  as a function of  $\tau$  (**inner loop**), and for each embedding cycle, a value of  $FNN$  is calculated as a function of  $m$  (**outer loop**). The first allows for an optimal  $\tau$  selection, while the later sets the optimal  $m$ , by the fraction of  $FNN$  points dropping to zero.

The core of the proposed  $N$  measure algorithm is: consider a matrix of  $n$  measurements on  $k$  variables,  $1 \leq k \leq d$ ; then, **1**) for each  $k$ -dimensional point  $x_{(u,k)}$ , where  $1 \leq u \leq n$ , that is, for each row in the  $(n \times k)$  measurements matrix, estimate its nearest neighbor  $y_{(v,k)}$ ; **2**) calculate the Euclidean distance between them,  $dist_1 = \sqrt{\sum_{j=1}^k (x_{(u,j)} - y_{(v,j)})^2}$ ; **3**) consider both points one sampling unit ahead,  $x_{(u+1,k)}$  and  $y_{(v+1,k)}$ ; **4**) calculate the new Euclidean distance between them,  $dist_2 = \sqrt{\sum_{j=1}^k (x_{(u+1,j)} - y_{(v+1,j)})^2}$ ; **5**) estimate the ratio  $\frac{dist_2}{dist_1}$ ; and **6**) estimate the fraction of points  $N$  that have a ratio  $\geq 10$ ; this threshold value, though heuristically set, is justified by numerical studies [12] and has low parametric sensitivity.

Two data sets out of a case study, the Lorenz system [14], will be used to illustrate the proposed procedure and to compare it to the conventional use of  $I$  based selection of fixed time delays. The first data set (*LorX*) is the  $x$ -coordinate of the Lorenz system of differential equations  $\dot{x} = \sigma(y - x)$ ,  $\dot{y} = x(\rho - z) - y$ ,  $\dot{z} = xy - \beta z$ , with parameters  $\sigma = 10$ ,  $\rho = 28$ ,  $\beta = 8/3$ . These equations were numerically integrated with a  $4 - 5^{th}$  order Runge-Kutta algorithm and sampled at  $\delta = 0.01$  intervals. Transients were removed. The

second data set ( $LorX\eta$ ) is a noise-contaminated version of  $LorX$  with Gaussian white noise of mean zero and variance one, used to access the effect of noise in the time delay selection and to consequently illustrate the behavior of the method under circumstances closer to the experimental reality, even more so for biological systems. Each data set includes a total of 8000 points,  $(\frac{1}{8})^{th}$  of which is plotted in Fig. 1.

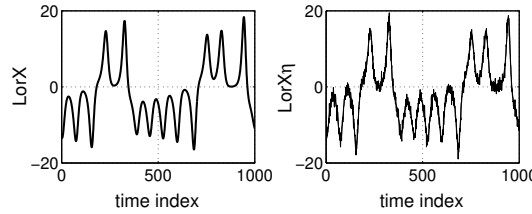


FIG. 1: Part of the two data sets used: noise-free  $x$ -coordinate of the Lorenz system ( $LorX$ ), and  $LorX$  contaminated with Gaussian white noise of mean 0 and variance 1 ( $LorX\eta$ ).

Concerning the first part of the phase space reconstruction problem, the  $\tau$ -selection profiles for the first embedding cycle are displayed in Fig. 2. Solid lines indicate the output from the  $N$  measure and dashed lines the output from  $I$ . The profiles for  $LorX$  [Fig. 2(a)] and  $LorX\eta$  [Fig. 2(b)] are displayed on the upper panel. On the lower panel, zoomed out versions of those same profiles are plotted to document behavior beyond dynamic coupling. A circle indicates  $\tau$ -selection as the first minimum of  $N$  and  $I$ . An arrow indicates the global minimum for  $N$  [Fig. 2(a) and Fig. 2(c), solid line] and that same value for the  $LorX\eta$  case [Fig. 2(b) and Fig. 2(d), solid line]. The interpretation of this figure will be clearer after also examining the profiles for the second embedding cycle, displayed in Fig. 3. As before, solid lines indicate the output from  $N$  and dashed lines indicate the output from  $I$ . The profiles for  $LorX$  [Fig. 3(a)] and  $LorX\eta$  [Fig. 3(b)] are displayed on the upper panel. Still as before, on the lower panel, zoomed out versions of those same profiles are plotted to document behavior beyond dynamic coupling. An asterisk indicates  $\tau$  values selected in the first embedding cycle for  $N$  and  $I$  (Fig. 2). A circle indicates  $\tau$ -selection for the second embedding cycle, again following the first minimum criterion. An arrow indicates the global minimum for  $N$  [Fig. 2(a) and Fig. 2(c), solid line].

Three main conclusions can be drawn from examining the  $\tau$ -selection profiles for the first two embedding cycles (Fig. 2 and Fig. 3). The first is that only  $N$  retains the inverse relationship with structure disclosure, that is, unlike  $I$ ,  $N$  values return to higher levels

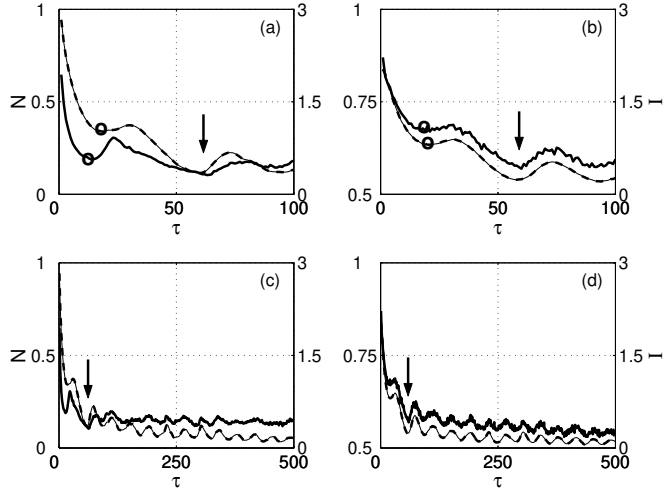


FIG. 2: Profiles for  $\tau$  selection in the first embedding cycle. Solid lines represent the  $N$  measure and dashed lines the  $I$  measure. Upper panel: (a)  $LorX$  and (b)  $LorX\eta$ . Lower panel: profiles beyond dynamic coupling for (c)  $LorX$  and (d)  $LorX\eta$ . A circle indicates the first minimum for  $N$  and  $I$ . An arrow indicates the global minimum for  $N$  [(a) and (c), solid line] and that same value for the noisy profile [(b) and (d), solid line].

when the time delay is too long for dynamical coupling to be retained [Fig. 2(c) and Fig. 3(c)]. This interception point is the global minimum of  $N$  [arrow symbols, Fig. 2(c) and Fig. 3(c)] and suggests an upper limit for the efficient selection of  $\tau$ , beyond which statistical independence reflects dynamic decoupling. This first observation provides a strong argument to why  $N$  should be preferred over  $I$  as a measure for selecting time delays. The effect of noise will be addressed below.

The second observation is that the profiles in both embedding cycles are strikingly different, independently of using  $N$  or  $I$ . This observation lends weight to the argument that reusing the time delay from the previous embedding cycle (circle symbols in Fig. 2 and asterisk symbols in Fig. 3), is not an efficient procedure. Quite the opposite, the values of both  $N$  and  $I$  for the second embedding cycle (asterisk symbols, Fig. 3) peak exactly for the  $\tau$  values selected previously (circle symbols, Fig. 2). This peaking was consistently observed not only for the data sets analyzed here, but also for other systems, such as the Rössler attractor [15], not shown here for space constraints. The actual gain in efficiency by allowing different time delays for consecutive embedding cycles is verified in the second part of the phase space reconstruction problem, and documented for  $LorX$  in Fig. 4, where

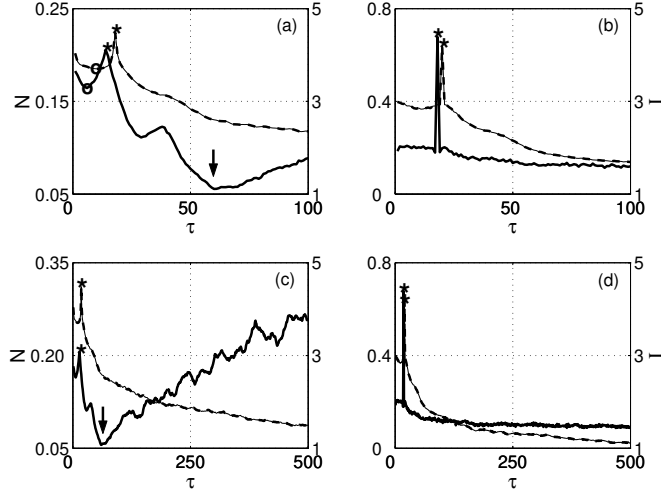


FIG. 3: Profiles for  $\tau$  selection in the second embedding cycle. Solid lines represent the  $N$  measure and dashed lines the  $I$  measure. Upper panel: (a)  $LorX$  and (b)  $LorX\eta$ . Lower panel: profiles beyond dynamic coupling for (c)  $LorX$  and (d)  $LorX\eta$ . An asterisk indicates  $\tau$  values selected in the first embedding cycle for  $N$  and  $I$  (Fig. 2). A circle indicates the first minimum for  $N$  and  $I$ . An arrow indicates the global minimum for  $N$ [(a) and (c), solid line].

the fraction of  $FNN$  is plotted as a function of  $m$ . The  $FNN$  algorithm is similar to the  $N$  algorithm explained before (see [12] for a more comprehensive explanation). By examining Fig. 4 it is clear that by using the  $N$  measure and allowing for different time delays (thick solid line), to contrast with the conventional use of  $I$  and fixed time delays (dashed line), the reconstruction is more efficient. This implies that, although both  $N$  and  $I$  suggest  $m = 3$  as the optimal embedding dimension, the percentage of  $FNN$  when  $m = 2$  is lower for  $N$  (thick solid line) than for  $I$  (dashed line), establishing the former as the most efficient. It is also noteworthy that using the global minimum of  $N$  (thin solid line) would be a suboptimal choice. Not only the percentage of  $FNN$  for each  $m$  is higher than in either of the previous cases, as  $m = 3$  is not sufficient for the reconstruction. This further confirms the importance of the global minimum as a criterion for upper-limiting the region where the selection of time delays should be made. The relevance of this boundary will be particularly valuable when analyzing noisy time series, as discussed below.

A third observation from the  $\tau$ -selection profiles, particularly clear in Fig. 3, refers to the disruptive effect of noise. Though the noise contamination of  $LorX\eta$  only mildly affects results for the first embedding cycle [Fig. 2(b) and Fig. 2(d)], where the first and the global

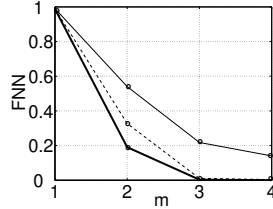


FIG. 4: Profiles for  $m$  selection for  $LorX$  using the  $FNN$  algorithm. The thicker solid line represents using a vector of  $\tau$  values, by selecting the first minima of  $N$  in each embedding cycle. The dashed line represents a fixed  $\tau$  value, selected as the first minimum of  $I$ . The thinner solid line represents using a  $\tau$  value selected as the global minimum of  $N$ .

[from the noise-free  $LorX$ , Fig. 2(c)] minima are still identifiable, it has a more severe effect on the second embedding cycle [Fig. 3(b) and Fig. 3(d)]. We suggest a heuristic to cope with this effect, illustrated for different noise contamination levels. Fig. 5 comprises six  $N$  profiles (solid lines) for the second embedding cycle for noise-free  $LorX$  [Fig. 5(a), as in Fig. 3(a)] and for  $LorX\eta$  [Fig. 5(b)] contaminated with Gaussian white noise of mean 0 and variance (A) 0.05, (B) 1 [as in Fig. 3(b)], (C) 2, (D) 3, and (E) 5. As before (Fig. 3), all curves peak exactly at the  $\tau$  value selected in the first embedding cycle (Fig. 2), and therefore that  $\tau$  value does not represent an optimal choice for this second embedding cycle. Furthermore, selecting a first minimum is no longer obvious. If two line-segments are fit over curves A to E [dashed lines, Fig. 5(b)], their intersection [arrow symbol, Fig. 5(b)] occurs approximately at the same  $\tau$  value as the global minimum for  $N$  [arrow symbol, Fig. 5(a)]. This feature is an interesting guideline, for the global minimum, as discussed before, though being a suboptimal choice (Fig. 4), sets the upper limit for the selection of  $\tau$  (Fig. 2 and Fig. 3), and can with this heuristic be inferred.

In conclusion, the nearest neighbor measure proposed  $N$ , unlike mutual information  $I$ , retains the inverse relationship with structure disclosure. This is an extremely useful feature for analyzing noisy time series as it allows for the determination of an upper limit to an efficient selection of time delays. Secondly, the use of different time delays is shown to be more efficient than the conventional use of a fixed time delay set by the first minimum of mutual information.

This work was supported by grants SFRH/BD/1165/2000 and POCTI/1999/BSE/34794 from Fundação para a Ciência e a Tecnologia, Portugal, and by the National Heart, Lung

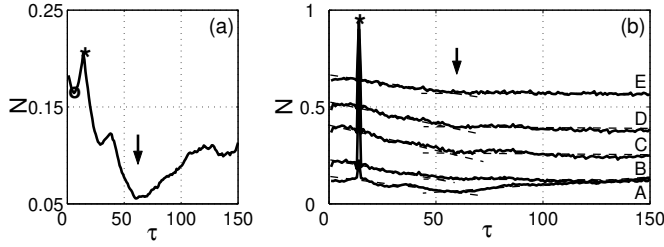


FIG. 5: Profiles for  $\tau$  selection in the second embedding cycle (solid lines) for: (a) *LorX* [as in Fig. 3(a)] and (b) *LorX* $\eta$  contaminated with Gaussian white noise of mean 0 and variance (A) 0.05, (B) 1 [as in Fig. 3(b)], (C) 2, (D) 3, and (E) 5. All curves peak at the  $\tau$  value selected in the first embedding cycle (see Fig. 3 for an explanation on asterisk and circle symbols). Two line-segments have been fit over curves A to E (dashed lines). Their intersection [(b), arrow symbol] occurs approximately at the same  $\tau$  value as the global minimum for  $N$  [(a), arrow symbol].

and Blood Institute (NIH) Proteomics Initiative through contract N01-HV-28181 (D Knapp, PI).

---

\* [spinto@itqb.unl.pt](mailto:spinto@itqb.unl.pt)

- [1] H. Kantz and T. Schreiber, *Nonlinear Time Series Analysis* (Cambridge University Press, Cambridge, UK, 1997).
- [2] H. Abarbanel, *Analysis of Observed Chaotic Data* (Springer, New York, 1996).
- [3] *Chaos* **5** (1995).
- [4] H. Kantz, J. Kurths, and G. M.-K. (Eds.), *Nonlinear Analysis of Physiological Data* (Springer, Heidelberg, 1998).
- [5] E. Voit and J. Almeida, *Bioinformatics* **20**, 1670 (2004).
- [6] T. Sauer, J. Yorke, and M. Casdagli, *J. Stat. Phys.* **65**, 579 (1991).
- [7] M. Casdagli, S. Eubank, J. Farmer, and J. Gibson, *Physica* (Amsterdam) **51D**, 52 (1991).
- [8] F. Takens, *Dynamical Systems and Turbulence* (Springer-Verlag, Berlin, 1981), vol. 898 of *Lecture Notes in Mathematics*, pp. 366–381.
- [9] A. Fraser and H. Swinney, *Phys. Rev. A* **33**, 1134 (1986).
- [10] C. Shannon and W. Weaver, *The Mathematical Theory of Communication* (University of Illinois Press, Urbana, IL, 1967).

- [11] H. Sturges, *J. Amer. Statist. Assoc.* **21**, 65 (1926).
- [12] T. Schreiber, *Phys. Rev. Lett.* **85**, 461 (2000).
- [13] M. Kennel, R. Brown, and H. Abarbanel, *Phys. Rev. A* **45**, 3403 (1992).
- [14] E. Lorenz, *J. Atmos. Sci.* **20**, 130 (1963).
- [15] O. Rössler, *Z. Naturforsch.* **31**, 1168 (1976).